BMC Medical Imaging

RESEARCH

Open Access

Gd-EOB-DTPA enhanced MRI nomogram model to differentiate hepatocellular carcinoma and focal nodular hyperplasia both showing iso- or hyperintensity in the hepatobiliary phase

Hao-yu Mao[1†], Bin-qing Shen[2†], Ji-yun Zhang[3†], Tao Zhang[3], Wu Cai[4], Yan-fen Fan[1], Xi-ming Wang[1], Yi-xing Yu[1*] and Chun-hong Hu[1*]

Abstract

Background To develop and validate a nomogram model based on Gd-EOB-DTPA enhanced MRI for differentiation between hepatocellular carcinoma (HCC) and focal nodular hyperplasia (FNH) showing iso- or hyperintensity in the hepatobiliary phase (HBP).

Methods A total of 75 patients with 49 HCCs and 26 FNHs randomly divided into a training cohort ($n=52$: 34 HCC; 18 FNH) and an internal validation cohort ($n=23$: 15 HCC; 8 FNH). A total of 37 patients ($n=37$: 25 HCC; 12 FNH) acted as an external test cohort. The clinical and imaging characteristics between HCC and FNH groups in the training cohort were compared. The statistically significant parameters were included into the FAE software, and a multivariate logistic regression classifier was used to identify independent predictors and establish a nomogram model. Receiver operating characteristic (ROC) curves were used to evaluate the prediction ability of the model, while the calibration and decision curves were used for model validation. Subanalysis was used to compare qualitative and quantitative characteristics of patients with chronic hepatitis and cirrhosis between the HCC and FNH groups.

Results In the training cohort, gender, age, enhancement rate in the arterial phase (AP), focal defects in uptake were significant predictors for HCC showing iso- or hyperintensity in the HBP. In the training cohort, area under the curve (AUC), sensitivity and specificity of the nomogram model were 0.989(95%CI: 0.967-1.000), 97.1% and 94.4%. In the internal validation cohort, the above three indicators were 0.917(95%CI: 0.782-1.000), 93.3% and 87.5%. In the external test cohort, the above three indicators were 0.960(95%CI: 0.905-1.000), 84.0% and 100.0%. The results of subanalysis

†Hao-yu Mao, Bin-qing Shen and Ji-yun Zhang contributed equally to this work.

*Correspondence:
Yi-xing Yu
yuyixing@163.com
Chun-hong Hu
sdhuchunhong@sina.com

Full list of author information is available at the end of the article

showed that age was the independent predictor in the patients with chronic hepatitis and cirrhosis between HCC and FNH groups.

Conclusions Gd-EOB-DTPA enhanced MRI nomogram model may be useful for discriminating HCC and FNH showing iso- or hyperintensity in the HBP before surgery.

Keywords Carcinoma, Hepatocellular, Focal nodular hyperplasia, Magnetic resonance imaging, Nomogram

Background

Liver cancer is the fifth most common cancer and the second leading cause of malignant death in Asia and the third leading cause of cancer-related deaths globally [1, 2], hepatocellular carcinoma (HCC) is the predominant histological subtype of liver cancer, accounting for 90 percentile of primary liver cancer [3], Gd-EOB-DTPA enhanced MRI is a commonly used imaging procedure to identify HCC, which typically shows "wash in" in the arterial phase (AP), "wash out" in the portal phase (PP), and hypointensity in the hepatobiliary phase (HBP) [4]. On the other hand, focal nodular hyperplasia (FNH) is a benign lesion of hepatocytic hyperplasia that arises in a normal or nearly normal live background, a typical FNH is an isolated, unencapsulated mass with a "radial" fibrous scar in the center and shows iso- or hyperintensity in the HBP [5, 6]. However, some HCCs [7–12] do not always reveal the typical hemodynamic pattern, which making it more challenging to diagnose well-differentiated HCC with conventional imaging procedure. Due to the overexpression of anion-transporting polypeptide of well-differentiated HCC, the lesion can take up specific contrast agents and shows iso- or hyperintensity in the HBP [13], Meanwhile, approximately 10–12% of FNHs may not show iso- or hyperintensity in the HBP [14]. Therefore, it is difficult to differentiate well- differentiated HCC from FNH preoperatively by Gd-EOB-DTPA enhanced MRI.

Currently, there is limited research on the imaging characteristics that distinguish HCC from FNH showing iso- or hyperintensity.in the HBP. This study aimed to compare and analyze the clinical. qualitative and quantitative imaging characteristics of HCC and FNH showing iso- or hyperintensity in the HBP based on Gd-EOB-DTPA enhanced MRI, in order to establish a nomogram model to improve the differentiation accuracy.

Materials and methods

Study sample

The institutional Ethics Review Board of the three hospitals approved this retrospective study and waived the requirement for written informed consent.

In this study, patients admitted to the three departments of Radiology from January 2015 to February 2023 were retrospectively collected. Inclusion criteria: ① Patients underwent Gd-EOB-DTPA enhanced MRI examination ten days before surgery; ② The lesions showed iso- or hyperintensity in the HBP; ③ The lesions were confirmed as HCC or FNH by postoperative pathology and immunohistochemistry; ④ If there were two or more lesions, the largest one was selected. Exclusion criteria: ① There were the artifacts in the images, which affected the observation of the lesions; ② Clinical data were incomplete. A total of 112 patients (72 men and 40 women, mean age 53 years, range 19–86 years) were included in this study, including 74 cases of HCC and 38 cases of FNH.

75 patients from the departments of Radiology of the First and Second Affiliated Hospital of Soochow University were randomly divided into the training and internal validation cohorts in a ratio of 6:4. 37 patients from the department of Radiology of the Affiliated Nantong Hospital 3 of Nantong University were used as external test cohort.

MRI acquisition

Before the examinations, the patients were given breathing training to ensure the quality of images. The scan was performed at the end of exhalation, with the center line setting at the lower margin of xiphoid process. MRI examinations were performed using a 3.0 T magnetic resonance scanner. The specific machines included Simens Magnetom Skyra 3.0T MRI (Siemens, Germany), GE Medical Systems 3.0T MRI (GE, USA) and Philips Medical Systems 3.0T MRI (Philips Netherlands) imaging system], a 16-channel phased array body coil, and a high-pressure syringe. Scanning sequence and parameters: ① T1-weighted imaging (T1WI) : repetition time (TR) 3.70～4.50 ms, echo time (TE) 1.20～1.90 ms, layer thickness 3.50～5.00 mm, field of view, FOV) 260 mm×320 mm～480 mm×480 mm; ② T2-weighted imaging (T2WI) : TR 4 000～6 000ms, TE 70～100 ms, layer thickness 7.50～9.00 mm, layer thickness 8.45～9.60 mm, FOV 260 mm×320 mm～512 mm×512 mm. ③ T1WI multiphase enhanced scanning: Simens Magnetom Skyra 3.0T MRI (Siemen, Germany), GE Medical Systems 3.0T MRI (GE, USA) and Philips Medical Systems 3.0T MRI (Philips, Netherlands) imaging systems respectively used 3D VIBE T1WI, BH Ax LAVA+C and mDIXON-W-dyn sequence, TR 2.90～4.20ms, TE 1.50～1.96ms, layer thickness 3.50～5.00 mm. FOV 260 mm x 320 mm～512 mm x 512 mm. A high-pressure syringe

was used to inject the contrast agent disodium gadolinate (Bayer Healthcare Co., LTD., Germany) into the cubitus vein mass with a dose of 0.025 mmol/kg and a flow rate of 1 ml/s. AP, PP, HBP images were acquired at 25～30s, 55～60s and 20 min after injection of the contrast agent, respectively.

Clinical characteristics

Preoperative routine laboratory examination results were collected, including age, gender, alanine aminotransferase (ALT≤50U/liter;>50U/liter), aspartate aminotransferase (AST≤40 U/liter;>40 U/liter), gamma-glutamyl transferase (GGT≤60 U/liter;>60 U/liter), alpha-fetoprotein (AFP≤25 μg/liter;>25 μg/ liter), viral hepatitis status and cirrhosis.

Qualitative and quantitative imaging characteristics

All MRI images were independently reviewed by two radiologists (with 5 and 10 years of experience in liver MRI imaging interpretation, respectively) using an image archiving and communication system (PACS, Neusoft v. 5.5, Shenyang, China). The two radiologists reached a consensus on the diagnosis of the images.

Qualitative imaging characteristics referred to the Liver Imaging Reporting and Data Statistics System (LI-RADS 2018 edition) [15], mainly including: ①maximum diameter: the maximum diameter was measured in the PP or equilibrium phase(EP); ② signal of the lesion: homogeneous or not; ③ margin of the lesion: smooth or not; ④ AP enhancement mode: non-rim AP hyperenhancement (APHE), rim AP hyperenhancement and mild enhancement; ⑤ non-peripheral "washout"; ⑥ enhancing capsule; ⑦ a hypointense ring: a hypointense ring surrounding an iso- or hyperintense lesion in the HBP; ⑧ focal defects in uptake: focal hypointense areas in the iso- or hyperintense lesion in the HBP.

Quantitative imaging characteristics mainly include: ① signal intensity(SI): the signal intensity of the lesion in the T2WI phase, pre-contrast (Pre) phase, AP, PP and HBP were respectively measured. The corresponding SIs were respectively expressed as SI_{T2}, SI_{Pre}, SI_{AP}, SI_{PP} and SI_{HBP}. ② Signal intensity ratio(SIR): SIR was calculated as the ratio of the signal intensity of the lesion to that of normal liver parenchyma, namely SI_{lesion} /SI_{liver}. These SIRs were respectively expressed as SIR_{T2}, SIR_{Pre}, SIR_{AP}, SIR_{PP} and SIR_{HBP}. ③ enhancement rate in the AP: enhancement rate in the AP =(SI_{AP}-SI_{Pre})/SI_{Pre}. Each measurement avoided the areas of vessels, bleeding, cystic degeneration and necrosis as much as possible. The measurement of the lesion was carried out at the largest level as far as possible. The area of the region of interests (ROIs) of normal liver parenchyma was 200mm^2, each ROI was measured 3 times and took average.

Statistical analysis

Statistical analyses were performed using SPSS 26.0, FAE software (version 0.5.2, https://github.com/salan668/FAE) and R software (version 4.1.3, https://www.r-project.org/).

The independent-sample t test or Mann-Whitney U test was performed to compare quantitative parameters and the chi-square test was used to compare qualitative characteristics. The Shapiro–Wilk test was used to test the normality of the data. Continuous variables were reported as the mean±standard deviation or median with interquartile range (IQR). Categorical variables were reported as frequency.

All quantitative parameters were nomalized by Z-score. Based on the training cohort, clinical qualitative and quantitative imaging characteristics selected by univariable analysis and RFE were tested for collinearity. Characteristics with high collinearity (pearson correlation coefficient>0.8) were deleted, the 10-fold cross-validation was carried out. The independent predictors were identified by logistic regression classifier. The above steps were implemented in FAE software.

Rms and rmda packages of R software were used to construct the nomogram model, calibration and decision curves. The discrimination efficiency of the nomogram model was assessed by the area under the receiver operating characteristic (ROC) curve (AUC) and calibration curve. A P value<0.05 (two-tailed) was considered statistically significant.

Results

Basic clinical characteristics analysis

In the training cohort, the differences of Gender, AST>40U/L, HBV(+), cirrhosis(+) and age were statistically significant between HCC and FNH groups(all $P<0.05$); there were no significant differences in ALT, GGT and AFP between the two groups (all $P\geq0.05$) (Table 1).

In the internal validation cohort, the differences of AFP>25 μg/L and age were statistically significant between HCC and FNH groups (all $P<0.05$); there were no significant differences in gender, ALT, AST, GGT, HBV and cirrhosis between the two groups (all $P\geq0.05$) (Table 1).

There were no significant differences in age, gender, ALT, AST, GGT, AFP, HBV, and cirrhosis between training and internal validation cohorts (all $P>0.05$) (Table 1).

Qualitative and quantitative imaging characteristics analysis

All the qualitative (Figs. 1 and 2) and quantitative characteristics were analyzed by univariable analysis.

In the training cohort, the proportion of non-peripheral "wash out", enhancing capsule and focal defects in

Table 1 Basic clinical characteristics of the patients in the training and internal validation cohorts

Characteristic	Training cohort ($n=52$)			Internal validation cohort ($n=23$)			
	HCC ($n=34$)	FNH ($n=18$)	*P* value	HCC ($n=15$)	FNH ($n=8$)	*P* value	**P* value
Age, years	64.24 ± 10.49	31.28 ± 9.79	< 0.001	59.27 ± 13.93	34.75 ± 11.21	< 0.001	0.646
Gender			< 0.001			0.074	0.126
Male	29	5		9	1		
Female	5	13		6	7		
ALT(U/liter)			0.179			0.122	1.000
≤ 50	24	16		10	8		
>50	10	2		5	0		
AST(U/liter)			0.004			0.257	0.270
≤ 40	19	17		11	8		
>40	15	1		4	0		
GGT(U/liter)			0.392			0.086	0.323
≤ 60	16	11		7	7		
>60	18	7		8	1		
AFP(μg/liter)			0.081			0.019	0.057
≤ 25	27	18		7	8		
>25	7	0		8	0		
HBV			0.006			0.052	0.606
(-)	16	16		8	8		
(+)	18	2		7	0		
Cirrhosis			0.017			0.052	0.450
(-)	16	15		8	8		
(+)	18	3		7	0		

**P* value represents the comparison between training and internal validation cohorts

ALT = alanine aminotransferase; AST = aspartate aminotransferase; GGT = gamma glutamyl transferase; HBV = Hepatitis B virus; AFP = alpha-fetoprotein

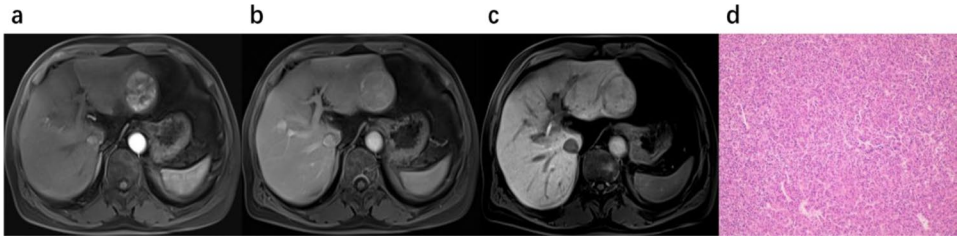

Fig. 1 Gd-EOB-DTPA enhanced MRI images of a patient with histological HCC in left lobe of liver. (**a**)The tumor shows non-rim hyperenhancement in the AP. (**b**) The degree of enhancement is decreased in the PP, namely non-peripheral "washout", and there is an enhancing capsule surrounding the tumor. (**c**) The tumor shows iso- or hyperintensity and focal hypointense areas in the iso- or hyperintense areas in the HBP. (**d**) Pathological findings of highly differentiated hepatocellular carcinoma (original magnification 40×)

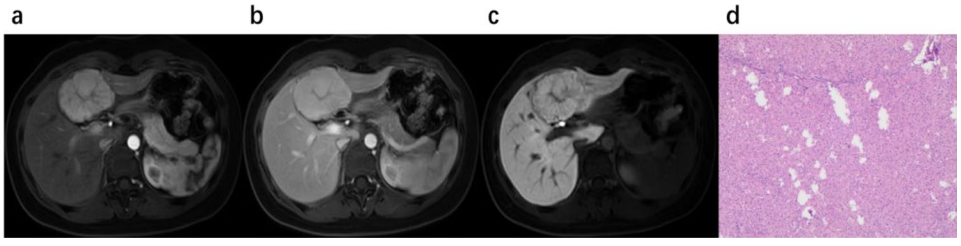

Fig. 2 Gd-EOB-DTPA enhanced MRI images of a patient with histological FNH in left lobe of liver. (**a**)The tumor shows non-rim hyperenhancement in the AP. (**b**) The tumor shows continuous enhancement in the PP. (**c**) The tumor shows iso- or hyperintensity in the HBP. (**d**) Pathological findings of focal nodular hyperplasia (original magnification 40×)

uptake showing in the HCC group were higher than that in the FNH group [38.2% (13/34) vs. 0% (0/18), $P=0.002$; 47.1% (16/34) vs. 0% (0/18), $P<0.001$; 67.6% (23/34) vs. 11.1% (2/18), $P<0.001$]. There were no significant differences in the maximum diameter, well-distributed signal, smooth margin, AP enhancement mode and a hypointense rim between the two groups (Table 2).

The results of quantitative imaging characteristics analysis in the training cohort showed that SIR_{AP} and enhancement rate in the AP in the FNH group were higher than those in the HCC group (1.66±0.27 vs. 1.44±0.37, $P=0.029$; 1.23±0.48 vs. 0.61±0.42, $P<0.001$). There were no significant differences in SI_{T2}, SIR_{T2}, SI_{Pre}, SIR_{Pre}, SI_{AP}, SI_{PP}, SIR_{PP}, SI_{DP} and SIR_{DP} between the two groups (Table 2).

Establishment and evaluation of nomogram model

The result of logistic regression showed that gender, age, enhancement rate in the AP and focal defects in uptake were the independent predictors for differentiating HCC from FNH showing iso- or hyperintensity in the HBP. Gd-EOB-DTPA enhanced MRI nomogram model was

Table 2 Analysis of qualitative and quantitative imaging characteristics of the patients between HCC and FNH groups in the training cohort

	HCC ($n=34$)	FNH ($n=18$)	t/Z/c^2	*P* value
Qualitative Characteristics				
Maximum diameter(cm)			0.617	0.562
≤5 cm	19	8		
> 5 cm	15	10		
Well-distributed signal in lesion			3.748	0.068
No	26	9		
Yes	8	9		
Smooth margin of lesion			0.088	0.767
No	5	4		
Yes	29	14		
AP enhancement mode			5.155	0.063
Non-rim AP hyperenhancement	22	17		
Rim AP hyperenhancement	2	0		
Mild enhancement	10	1		
Non-peripheral "washout"			-	0.002
No	21	18		
Yes	13	0		
Enhancing capsule			-	< 0.001
No	16	18		
Yes	18	0		
A hypointense rim			< 0.001	1.000
No	33	17		
Yes	1	1		
Focal defects in uptake			12.890	< 0.001
No	11	16		
Yes	23	2		
Quantitative Characteristics				
SI_{T2}	225.00 (128.75,378.50)	133.50 (96.50,419.50)	-1.346	0.178
SIR_{T2}	1.70(1.37,2.64)	1.48(1.30,1.90)	-1.247	0.211
SI_{Pre}	247.01 ± 106.29	228.84 ± 110.47	-0.579	0.566
SIR_{Pre}	0.89(0.75,0.99)	0.86(0.84,0.95)	-0.289	0.773
SI_{AP}	388.94 ± 171.89	498.86 ± 250.60	1.866	0.068
SIR_{AP}	1.44 ± 0.37	1.66 ± 0.27	2.250	0.029
Enhancement rate in the AP	0.61 ± 0.42	1.23 ± 0.48	4.817	< 0.001
SI_{PP}	375.00 (290.25,579.25)	472.50 (269.25,643.60)	-1.106	0.269
SIR_{PP}	1.14 ± 0.29	1.17 ± 0.16	0.388	0.699
SI_{HBP}	381.50 (258.25,499.25)	514.91 ± 257.32	-1.154	0.248
SIR_{HBP}	0.98(0.88,1.13)	1.08 ± 0.16	-1.299	0.194

Pre = pre-contrast; AP = arterial phase; PP = portal venous phase; HBP = hepatobiliary phase; SI = signal intensity; SIR = signal intensity ratio; Enhancement rate in the AP = $(SI_{AP}-SI_{Pre})/SI_{Pre}$

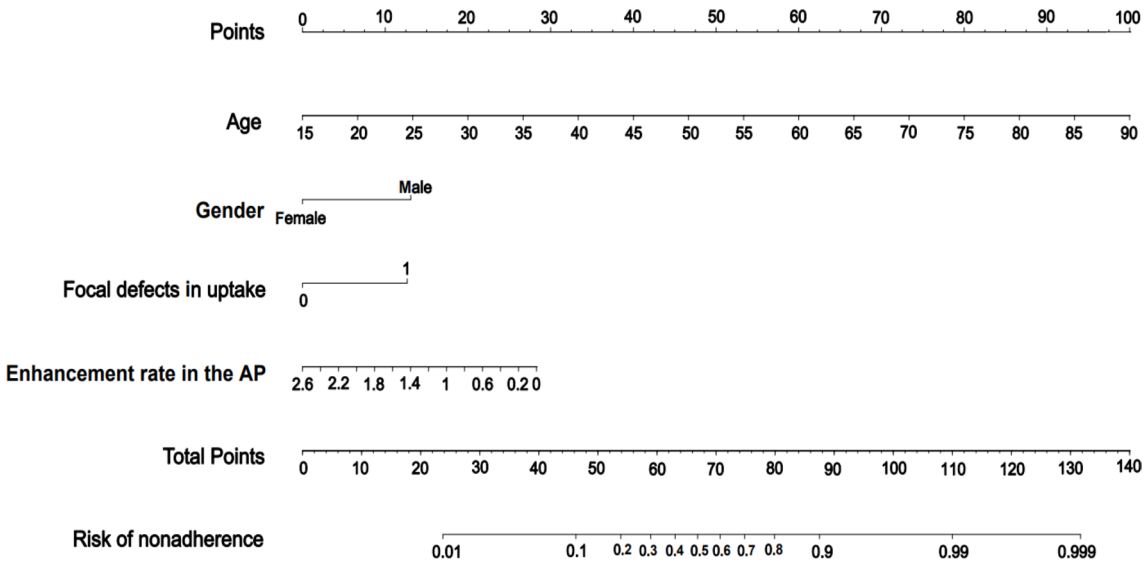

Fig. 3 The Gd-EOD-DTPA enhanced MRI nomogram model for distinguishing HCC from FNH showing iso- or hyperintensity in the HBP. According to the age, gender, enhancement rate in the AP and focal defects in uptake of each patient, the vertical line between each indicator and the score of the column chart was drawn to obtain the score value of each indicator. Then, the score of these indicators was added to get the total score. Finally, the vertical line between the total score and the risk of HCC showing iso- or hyperintensity in the HBP of the nomogram model was drawn to obtain the predicted probability of HCC showing iso- or hyperintensity in the HBP

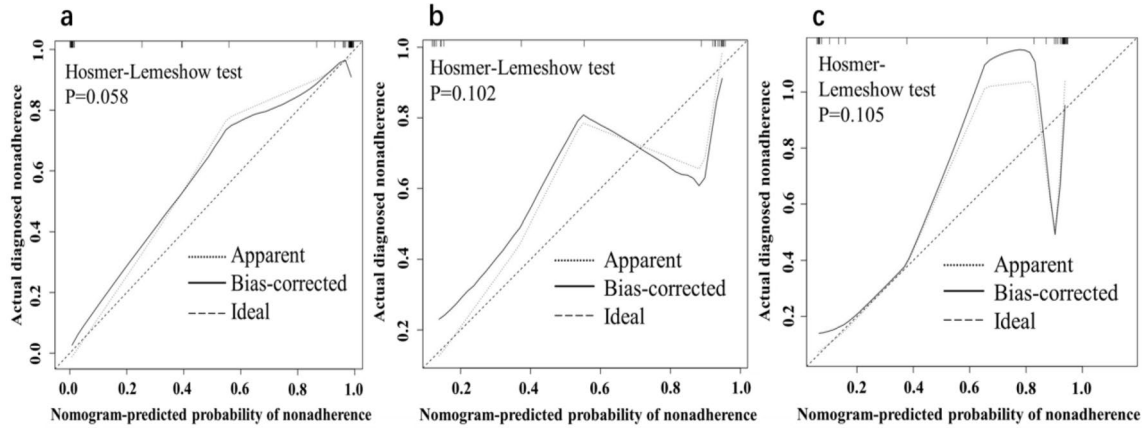

Fig. 4 Calibration curves of the Gd-EOD-DTPA enhanced MRI nomogram model for distinguishing HCC from FNH showing iso- or hyperintensity in the HBP. (**a**) Training cohort. (**b**) Internal validation cohort. (**c**) External test cohort

successfully established (Fig. 3). The calibration prediction curve fitted well with the standard curve and the *P* values of Hosmer-Lemeshow test in the training, internal validation and external test cohorts were 0.058, 0.102 and 0.105, indicating that the nomogram model had good discriminative efficiency (Fig. 4). The decision curves showed that the nomogram model had a high overall net income and clinical decision effectiveness (Fig. 5). In the training cohort, the AUC (95%CI), sensitivity and specificity of the nomogram model were 0.989(0.967-1.000), 97.1% and 94.4%. In the internal validation cohort, the above three indicators were 0.917(0.782-1.000), 93.3% and 87.5%. In the external test cohort, the above three indicators were 0.96(0.905-1.000), 84.0% and 100.0%, respectively (Fig. 6).

Subanalysis in the patients with chronic hepatitis and cirrhosis

A total of 58 chronic hepatitis and cirrhosis patients (47 men and 11 women) were included in the subanalysis, including 53 cases of HCC and 5 cases of FNH. The results of univariate analysis showed that enhancement rate in the AP in the FNH group was higher than that of the HCC group (1.57±0.80 vs. 0.58[0.29,1.12], $P=0.021$), and age in the HCC group was higher than that of the FNH group (60.45±10.13 vs. 39.80±11.45, $P<0.001$). Multivariate logistic regression analysis showed that age

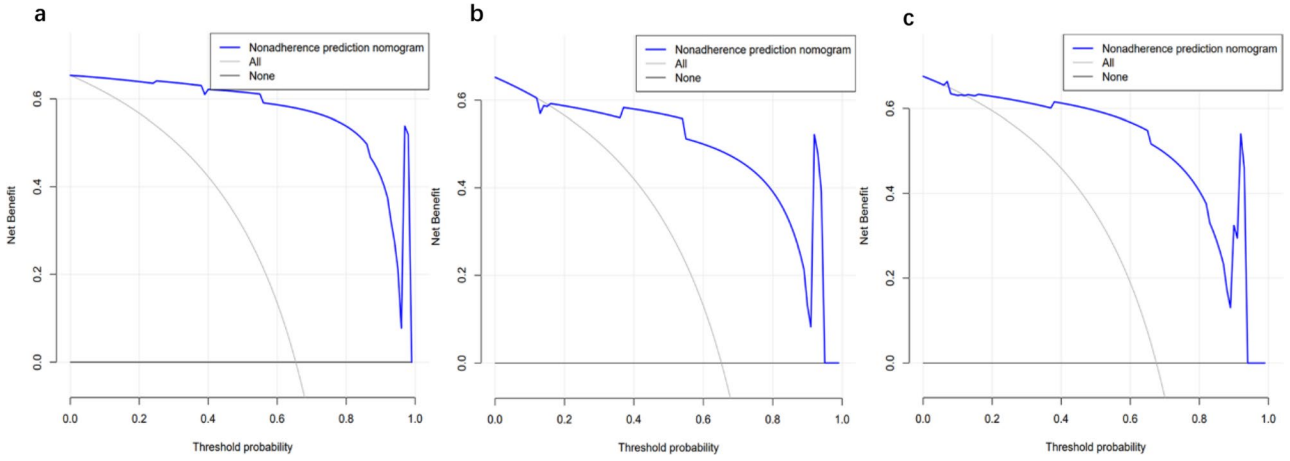

Fig. 5 Decision curves of the Gd-EOD-DTPA enhanced MRI nomogram model for distinguishing HCC from FNH showing iso- or hyperintensity in the HBP. (**a**) Training cohort. (**b**) Internal validation cohort. (**c**) External test cohort

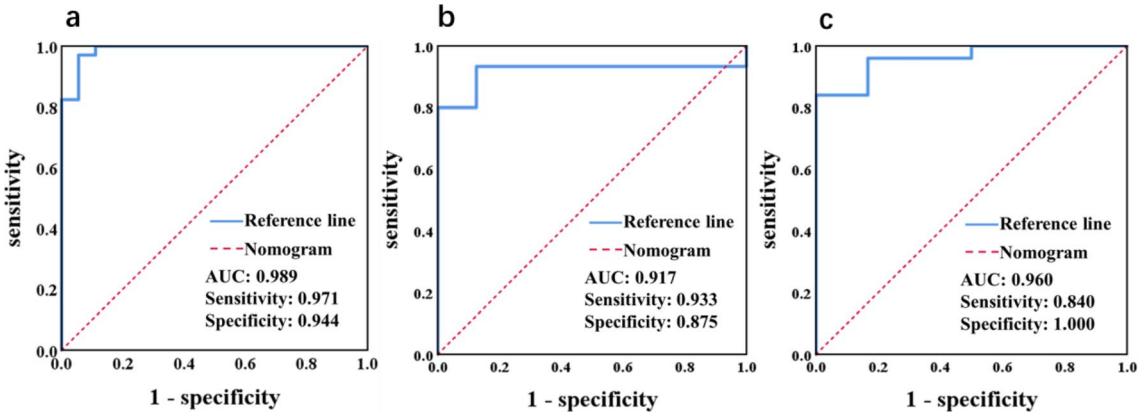

Fig. 6 ROC curves of the Gd-EOD-DTPA enhanced MRI nomogram model for distinguishing HCC from FNH showing iso- or hyperintensity in the HBP. (**a**) Training cohort. (**b**) Internal validation cohort. (**c**) External test cohort

was an independent predictor in distinguishing HCC from FNH both showing iso- or hyperintensity in the patients with chronic hepatitis and cirrhosis (Table 3).

Discussion

HCC, as a kind of malignant tumor with poor prognosis, the most effective treatment is surgical resection, and early detection and early treatment is essential. However, well-differentiated HCC is not typical in both clinical symptoms and imaging findings [16]. Existing studies have shown that FNH is polyclonal tumor-like lesion and does not undergo haemorrhage or malignant transformation [17] and regular follow-up is generally required. Therefore, accurate prediction of HCC showing iso- or hyperintensity in the HBP before surgery is crucial for clinical decision. In recent studies, radiomics models have been used to predict HCC and FNH before surgery. Ding et al. [9] investigated the identification of HCC and FNH in non-cirrhotic settings, multivariate logistic regression analysis was used to construct radiomics, clinical, and clinical-radiomics combined model. The results showed that the combined model had high differential efficiency and provided a non-invasive quantitative method for distinguishing HCC and FNH in non-cirrhotic settings. However, this study did not analyze the qualitative and quantitative imaging characteristics of HCC and FNH. In this study, gender, age, enhancement rate in the AP, and focal defects in uptake were independent predictors for differentiating HCC from FNH showing iso- or hyperintensity in the HBP. The nomogram model constructed by combining the above four independent predictors had an AUC of 0.917, sensitivity and specificity of 93.3% and 87.5% in the internal validation cohort, and an AUC of 0.96, sensitivity and specificity of 84.0% and 100.0% in the external test cohort.

Based on clinical, qualitative and quantitative characteristics, such as gender, enhancement mode, morphological characteristics, signal intensity ratio, and so on, we found that HCC mostly occurs in middle-aged men, while FNH often occurs in young women, which is

Table 3 Analysis of qualitative and quantitative characteristics of patients with the Chronic Hepatitis and cirrhosis between HCC and FNH groups

	HCC($n=53$)	FNH($n=5$)	c^2/Z/t	*P* value	Multivariate logistic regression analysis	
					P value	OR (95%CI)
Qualitative Characteristics						
Gender			3.429	0.064	-	-
Male	45	2				
Female	8	3				
ALT(U/liter)			-	0.309	-	-
≤ 50	37	5				
>50	16	0				
AST(U/liter)			-	0.146	-	-
≤ 40	30	5				
>40	23	0				
GGT(U/liter)			2.700	0.100	-	-
≤ 60	24	4				
>60	29	1				
AFP(μg/liter)			-	0.309	-	-
≤ 25	37	5				
>25	16	0				
Maximum diameter(cm)			-	0.309	-	-
≤ 5 cm	37	5				
>5 cm	16	0				
Well-distributed signal in lesion			0.738	0.390	-	-
No	16	3				
Yes	37	2				
Smooth margin of lesion			-	1.000	-	-
No	45	5				
Yes	8	0				
AP enhancement mode			1.558	0.212	-	-
Non-rim AP hyperenhancement	37	4				
Rim AP hyperenhancement	6	0				
Mild enhancement	10	1				
Non-peripheral "washout"			-	0.053	-	-
No	25	5				
Yes	28	0				
Enhancing capsule			-	0.058	-	-
No	27	5				
Yes	26	0				
A hypointense rim			< 0.001	1.000	-	-
No	46	4				
Yes	7	1				
Focal defects in uptake			1.402	0.098	-	-
No	22	4				
Yes	31	1				
Quantitative Characteristics						
Age	60.45 ± 10.13	39.80 ± 11.45	-4.317	< 0.001	0.042	1.208(1.007 ~ 1.448)
SI_{T2}	245.03(182.48,387.09)	310.75 ± 184.78	-0.263	0.792	-	-
SIR_{T2}	0.91(0.83,1.05)	0.87(0.85.1.06)	-0.125	0.901	-	-
SI_{Pre}	261.00(135.50,472.55)	235.80 ± 127.84	-0.900	0.368	-	-
SIR_{Pre}	1.65(1.39,2.28)	1.66 ± 0.34	-0.319	0.750	-	-
SI_{AP}	411.00(292.00,655.00)	840.50 ± 664.61	-1.191	0.234	-	-
SIR_{AP}	1.42(1.27,1.62)	1.71 ± 0.43	-1.482	0.138	-	-
Enhancement rate in the AP	0.58(0.29,1.12)	1.57 ± 0.80	-2.313	0.021	0.360	0.293(0.021 ~ 4.049)
SI_{PP}	427.00(302.00,769.50)	778.48 ± 524.06	-1.011	0.312	-	-

Table 3 (continued)

	HCC($n=53$)	FNH($n=5$)	c^2/Z/t	*P* value	Multivariate logistic regression analysis	
					P value	OR (95%CI)
SIR_{PP}	1.08(0.98,1.27)	1.08 ± 0.13	-0.139	0.890	-	-
SI_{HBP}	392.00(265.50,625.50)	650.00 ± 492.67	-0.623	0.533	-	-
SIR_{HBP}	0.99(0.90,1.11)	0.90 ± 0.17	-1.233	0.217	-	-

ALT=alanine aminotransferase; AST=aspartate aminotransferase; GGT=gamma glutamyl transferase; AFP=alpha-fetoprotein; Pre=pre-contrast; AP=arterial phase; PP=portal venous phase; HBP=hepatobiliary phase; SI=signal intensity; SIR=signal intensity ratio; Enhancement rate in the AP=$(SI_{AP}-SI_{Pre})/SI_{Pre}$; OR=odds ratio; CI: confidence interval

consistent with clinical and epidemiological reports over the years. Hemodynamics shows that well-differentiated HCC is mostly supplied by portal vein or by both portal vein and hepatic artery, thus, the enhancement rate in the AP of HCC showing iso- or hyperintensity was lower than that of FNH in this study; This also indicates from the side that well-differentiated HCC does not show the typical high enhancement in the AP, and its degree of enhancement is usually lower. Compared with FNH, HCC is more likely to show focal defects in uptake, this may be due to the heterogeneity and atypia of malignant tumors, and there exists poorly-differentiated region in the whole well-differentiated lesion, which does not take up specific contrast agents and shows hypointensity in the HBP.

Furthermore, considering that in the background of chronic hepatitis and cirrhosis, cirrhotic nodules with contrast agent ingestion in the HBP are major problems in misdiagnosis, we conducted a subanalysis analysis in the patients with chronic hepatitis or cirrhosis among the subjects of this study. The results showed that age was an independent predictor for distinguishing HCC from FNH showing iso-or hyperintensity in these patients. However, other independent predictors such as gender, age, enhancement rate in the AP and focal defects in uptake were not statistically significant in the subanalysis, which differed from the results of the nomogram model. This discrepancy may be attributed to the reduced number of cases.

Varieties of nomogram models have been successfully applied in the study of clinical diseases, such as nomogram for predicting overall survival in patients with low-grade endometrial stromal sarcoma [18], prediction of tumor response via a pretreatment MRI radiomics-based nomogram in HCC treated with TACE [19], Nomogram established on account of Lasso-Cox regression for predicting recurrence in patients with early-stage hepatocellular carcinoma [20], and so on. Therefore, the nomogram model has important value in the research of liver diseases. At present, there are few reports about imaging characteristics on the identification of HCC and FNH showing iso- or hyperintensity.

Kitao Azusa et al. [21] analyzed the imaging findings of dynamic CT and Gd-EOB-DTPA MRI of hyperintense HCCs, FNHs and FNH-like nodules. The result showed that ADC ratio and arterial phase enhancement and washout pattern at dynamic CT were the independent predictor factors for differentiation between hyperintense HCC and FNH. Compared with Kitao's study, clinical and imaging characteristics were included in multivariate logistic regression analysis and a nomogram model was established in our study to display the results more intuitively. Moreover, our study is polycentric, and the established model is verified externally. Considering that the enhancement mode of the lesions on CT and MRI were similar except for the hepatobiliary specific phase, the imaging characteristics of CT enhancement were not included in our study.

In this study, a nomogram model based on clinical, imaging qualitative and quantitative characteristics was established to predict and identify HCC showing iso- or hyperintensity before surgery. The Gd-EOB-DTPA enhanced MRI nomogram model can obtain the probability of HCC occurrence through a simple addition operation, which is conducive to personalized prediction of each patient. The AUC of the internal and external test cohort is 0.917 and 0.960, indicating that the model has good identification efficiency.

Limitations

As a retrospective study with small sample size, we will continue to collect relevant cases in the future. Secondly, only the images of T1WI and T2WI phase, AP, PP and HBP were analyzed in this study, the other sequences, such as ADC and DWI, could be added later to improve the multi-parameter study.

Conclusion

The nomogram model shows high sensitivity and specificity in discriminating between HCC and FNH showing iso- or hyperintensity in the HBP in both training, internal and external test cohorts and has good generalization and repeatability. Therefore, it may help diagnose HCC showing iso- or hyperintensity in the HBP in preoperative individuals and assist clinicians in clinical decisions.

Abbreviations

AFP	Alpha-fetoprotein
ALT	Alanine aminotransferase
AP	Arterial phase
AST	Aspartate aminotransferase

AUC	Area under the receiver operating characteristic curve
Gd-EOB-DTPA	Gadolinium-ethoxybenzyl-diethylenetriamine pentaacetic acid
CI	Confidence interval
FNH	Focal nodular hyperplasia
GGT	Gamma glutamyl transferase
HBP	Hepatobiliary phase
HBV	Hepatitis B virus
HCC	Hepatocellular carcinoma
PP	portal venous phase
Pre	Pre contrast
ROC	Receiver operating characteristic
ROI	Region of interest
SI	Signal intensity
SIR	Signal intensity ratio

Acknowledgements
Not applicable.

Author contributions
MHY Conceptualization, Acquisition, analysis and interpretation of data, Writing of the original draft, ZJY Acquisition of data, Writing of the original draft, ZT and SBQ Acquisition of data, Investigation, CW Acquisition of data, Investigation, FYF Conceptualization, Methodology, WXM Conceptualization, Methodology, YYX Conceptualization, Methodology, Revision, HCH Conceptualization, Methodology, Revision. All authors read and approved the final manuscript.

Funding
Project of Suzhou Gusu Health Talents Program (GSWS2020003), The Natural Science Foundation of Jiangsu Higher Education Institutions of China(22KJB320022), Suzhou Science and Technology Plan Project (SKY2023146), National College Student Innovation and Entrepreneurship Training Program of Soochow University (202310285069Z).

Data availability
The datasets during this study are not publicly available, but are available from the corresponding author on reasonable request.

Declarations

Ethics approval and consent to participate
The institutional Ethics Review Board of the First Affiliated Hospital of Soochow University, the Second Affiliated Hospital of Soochow University and Affiliated Nantong Hospital 3 of Nantong University approved this retrospective study and waived the requirement for written informed consent.

Consent for publication
Not applicable.

Competing interests
The authors declare no competing interests.

Author details
[1]Department of Radiology, The First Affiliated Hospital of Soochow University, Suzhou, China
[2]School of Radiation Medicine and Protection, Soochow University, Suzhou, China
[3]Department of Radiology, Affiliated Nantong Hospital 3 of Nantong University, Nantong, China
[4]Department of Radiology, The Second Affiliated Hospital of Soochow University, Suzhou, China

Received: 1 May 2024 / Accepted: 29 July 2024
Published online: 12 August 2024

References

1. Sweed D, Sweed E, Moaz I, et al. The clinicopathological and prognostic factors of hepatocellular carcinoma: a 10-year tertiary center experience in Egypt. World J Surg Oncol. 2022;20(1):298.
2. Zhang CH, Cheng Y, Zhang S, Fan J, Gao Q. Changing epidemiology of hepatocellular carcinoma in Asia. Liver Int. 2022;42(9):2029–41.
3. Chidambaranathan-Reghupaty S, Fisher PB, Sarkar D. Hepatocellular carcinoma (HCC): epidemiology, etiology and molecular classification. Adv Cancer Res. 2021;149:1–61.
4. Raatschen HJ. Radiological diagnostic workup of liver tumors. Internist (Berl). 2020;61(2):123–30.
5. Oldhafer KJ, Habbel V, Horling K, et al. Benign liver tumors. Visc Med. 2020;36(4):292–303.
6. LeGout JD, Bolan CW, Bowman AW, et al. Focal nodular Hyperplasia and focal nodular hyperplasia-like lesions. Radiographics. 2022;42(4):1043–61.
7. Kawada N, Ohkawa K, Tanaka S, et al. Improved diagnosis of well-differentiated hepatocellular carcinoma with gadolinium ethoxybenzyl diethylene triamine pentaacetic acid-enhanced magnetic resonance imaging and Sonazoid contrast-enhanced ultrasonography. Hepatol Res. 2010;40(9):930–6.
8. Nie P, Yang G, Guo J, et al. A CT-based radiomics nomogram for differentiation of focal nodular hyperplasia from hepatocellular carcinoma in the non-cirrhotic liver. Cancer Imaging. 2020;20(1):20.
9. Ding Z, Lin K, Fu J, et al. An MR-based radiomics model for differentiation between hepatocellular carcinoma and focal nodular hyperplasia in non-cirrhotic liver. World J Surg Oncol. 2021;19(1):181.
10. Li W, Li R, Zhao X, et al. Differentiation of Hepatocellular Carcinoma from Hepatic Hemangioma and focal nodular hyperplasia using computed Tomographic Spectral Imaging. J Clin Transl Hepatol. 2021;9(3):315–23.
11. Hanaoka J, Shimada M, Utsunomiya T, et al. Huge focal nodular hyperplasia difficult to distinguish from well-differentiated hepatocellular carcinoma. Hepatol Res. 2012;42(7):727–31.
12. Lee MH, Kim SH, Park MJ, et al. Gadoxetic acid-enhanced hepatobiliary phase MRI and high-b-value diffusion-weighted imaging to distinguish well-differentiated hepatocellular carcinomas from benign nodules in patients with chronic liver disease. AJR Am J Roentgenol. 2011;197(5):W868–875.
13. Kitao A, Zen Y, Matsui O, et al. Hepatocellular carcinoma: signal intensity at gadoxetic acid-enhanced MR imaging–correlation with molecular transporters and histopathologic features. Radiology. 2010;256(3):817–26.
14. Zech CJ, Grazioli L, Breuer J, Reiser MF, Schoenberg SO. Diagnostic performance and description of morphological features of focal nodular hyperplasia in Gd-EOB-DTPA-enhanced liver magnetic resonance imaging: results of a multicenter trial. Invest Radiol. 2008;43:504–11.
15. Chernyak V, Fowler KJ, Kamaya A, et al. Liver Imaging reporting and data system (LI-RADS) version 2018: imaging of hepatocellular carcinoma in at-risk patients. Radiology. 2018;289:816–30.
16. Vernuccio F, Gagliano DS, Cannella R, Ba-Ssalamah A, Tang A, Brancatelli G. Spectrum of liver lesions hyperintense on hepatobiliary phase: an approach by clinical setting. Insights Imaging. 2021;12(1):8.
17. Khanna M, Ramanathan S, Fasih N, Schieda N, Virmani V, McInnes MD. Current updates on the molecular genetics and magnetic resonance imaging of focal nodular hyperplasia and hepatocellular adenoma. Insights Imaging. 2015;6:347–62.
18. Wu J, Zhang H, Li L, et al. A nomogram for predicting overall survival in patients with low-grade endometrial stromal sarcoma: a population-based analysis. Cancer Commun (Lond). 2020;40(7):301–12.
19. Kong C, Zhao Z, Chen W, et al. Prediction of tumor response via a pretreatment MRI radiomics-based nomogram in HCC treated with TACE. Eur Radiol. 2021;31(10):7500–11.
20. Wang Q, Qiao W, Zhang H, et al. Nomogram established on account of Lasso-Cox regression for predicting recurrence in patients with early-stage hepatocellular carcinoma. Front Immunol. 2022;13:1019638.
21. Kitao A, Matsui O, Yoneda N, et al. Differentiation between hepatocellular carcinoma showing hyperintensity on the hepatobiliary phase of Gadoxetic acid-enhanced MRI and focal nodular hyperplasia by CT and MRI. AJR Am J Roentgenol. 2018;211:347–57.

Publisher's Note